sustainability

MDPI

Article

Contributions of Biotic and Abiotic Factors to the Spatial Heterogeneity of Aboveground Biomass in Subtropical Forests: A Case Study of Guizhou Province

Tie Zhang [1], Guijie Ding [1,2], Jiangping Zhang [3] and Yujiao Qi [1,*]

[1] College of Forestry, Guizhou University, Guiyang 550025, China
[2] Institute for Forest Resources and Environment of Guizhou, Guiyang 550025, China
[3] Forest Surveying and Planning Institute of Guizhou Province, Guiyang 550003, China
* Correspondence: yjqi@gzu.edu.cn

Abstract: The spatial heterogeneity on a regional scale of forest biomass is caused by multiple biotic and abiotic factors. However, the contributions of biotic and abiotic factors to the spatial heterogeneity of forest biomass remain unclear. Based on the data of the National Forest Continuous Inventory (NFCI), digital elevation model (DEM), and meteorological data of Guizhou Province in 2015, we studied the spatial heterogeneity of the aboveground forest biomass in Guizhou province and evaluated the contribution rates of its influencing factors using Moran's *I*, semivariogram, distance-based Moran's eigenvector maps (dbMEMs), and variance partitioning. The results showed that the forest biomass in Guizhou province had strong spatial heterogeneity. Biotic and abiotic factors explained 34.4% and 19.2% of the spatial variation in forest biomass, respectively. Among the biotic factors, the average height of the stand had the greatest influence on forest biomass, while annual precipitation had the greatest influence on forest biomass among abiotic factors. Spatial factors only explained 0.7% of the spatial variation of forest biomass, indicating that the contribution of spatial factors can be explained by some measured abiotic factors. This study provided an effective approach to understand the underlying mechanisms of spatial allocation of forest biomass.

Keywords: forest aboveground biomass; driver analysis; variance partitioning; semivariogram; spatial autocorrelation

Citation: Zhang, T.; Ding, G.; Zhang, J.; Qi, Y. Contributions of Biotic and Abiotic Factors to the Spatial Heterogeneity of Aboveground Biomass in Subtropical Forests: A Case Study of Guizhou Province. *Sustainability* **2022**, *14*, 10771. https://doi.org/10.3390/su141710771

Academic Editors: Rui Manuel de Sousa Fragoso and Carlos Alberto Falcão Marques

Received: 15 July 2022
Accepted: 25 August 2022
Published: 29 August 2022

1. Introduction

Forest biomass is recognized to be a global climate observing system, and forests play an extremely important role in the carbon cycle in terrestrial ecosystems [1,2]. Accurate assessment of the temporal and spatial variations of forest biomass can provide an important scientific basis for managing forest resources to achieve sustainable development and have great significance for studying carbon cycles and sinks [3,4]. The data from the National Forest Continuous Inventory (NFCI) are an important basis on which to reflect national forest resources and forest management or to design an evidence-based forest policy at various scales; these data can also provide basic effective approaches for extracting forest resource information at national and regional scales [5,6]. Currently, many researchers have used the NCFI to evaluate the spatial and temporal distribution characteristics of forest biomass or carbon storage at different scales to clarify the dynamic changes and distribution of forest resources [7–9]. Forests have high spatial heterogeneity, which is defined as the complex and non-uniform spatial distribution caused by the combined effect of biotic and abiotic stress factors [10,11]. It is very important to clarify the effects of various factors on the spatial variation of forest biomass to understand the potential mechanisms for forest biomass changes and allocation at a large scale.

Forest biomass changes and distribution are controlled by multiple factors. Some studies have shown that biological factors such as diameter at breast height (DBH), stand

height, stand age, and stand density are the main factors affecting forest biomass [12–15]. Furthermore, large diameter trees are often used to support the effect of mass ratios of large trees within a community that regulate forest biomass changes [16]. Lutz et al. [17] further showed that the DBH was the major contributor to forest biomass of different boreal, temperate, and tropical forests derived from a global database. Another important theory is the niche complementarity hypothesis, which holds that species diversity increases forest biomass due to the complementary utilization of available resources by co-existing species in different ecological niches [18,19]. The factors interact more indirectly and affect forest biomass [20]. Xu et al. [12] reported that the stand density and stand age indirectly affected vegetation biomass by significantly influencing other factors (e.g., species diversity). The canopy density largely determined the structure and growth of the forest and was also an important driving factor in the accumulation of forest biomass [13,15]. In addition, forest biomass and its distribution are also related to abiotic factors such as topography, climatic factors, etc. It has been shown that the forest biomass of temperate and tropical forests is mainly limited by precipitation [14]. In small-scale regions, topography often affects the local microclimate. For example, elevation and slope can affect the distribution of forest biomass by influencing rainfall [12,21], solar radiation, wind speed, and soil type [13], while precipitation and temperature influence water and nutrient availability, thus influencing plant transpiration rates [18,22,23]. When these conditions are in the favorable range for plant growth, these factors increase forest biomass [16]. Furthermore, forest biomass also varies with logging [3], land use [24], wind [25], forest diseases [26], forest fires [27], etc. Generally, the spatial distribution of forests is accompanied by spatial autocorrelation, which refers to the statistical correlation between the spatial attribute values of geographical objects distributed in different spatial locations. The closer the distance is, the stronger the correlation between the two variables is. Spatial correlation and heterogeneity occur when the study area is large and correlated [28]. Spatial autocorrelation plays an important role in determining forest spatial heterogeneity [5,29]. In summary, the factors affecting the spatial heterogeneity of forest biomass can be divided into three categories: biotic factors, abiotic factors, and spatial autocorrelation. Most studies have determined the correlation between forest biomass and forest stand and abiotic factors based on regression analysis, while the contribution of biotic and abiotic factors to the spatial heterogeneity of forest biomass is rarely quantified.

Guizhou province, located upstream of the Yangtze and Pearl River waters, is situated in a subtropical plateau in a mountainous area. It is considered an important ecological security barrier area and a typical karst distribution region in China, with different types of karst landforms, which are one of China's famous natural World Heritage Sites [30]. Guizhou has many different kinds of plant species and the richest natural forest resources, including subtropical evergreen broad-leaved forests, tropical monsoon forests, mountain forests, cold temperate coniferous forests, subtropical coniferous forests, and secondary deciduous broad-leaved deciduous forests [6]. Therefore, quantifying the spatial distribution pattern of forest biomass and its key drivers in Guizhou province is of great significance for biodiversity conservation, ecological environment protection, and sustainable forest management in China and around the world. This study aimed to (1) analyze the spatial distribution pattern of forest biomass in Guizhou province; (2) evaluate the contribution of biotic and abiotic factors, as well as spatial autocorrelation, to the spatial heterogeneity of forest biomass.

2. Materials and Methods

2.1. Description of the Study Site

Guizhou province is located in southwest China (24°30′ N–29°13′ N and 103°31′ E–109°30′ E) (Figure 1). It covers an area of 176,128 km^2, of which 92.5% is mountainous and hilly, and the area of rocky desertification accounts for 17.1% of the total land area. It has an altitude/elevation of 137–2900 m (an average elevation of 1100 m) [30]. Guizhou province has a humid subtropical plateau mountain monsoon climate, which straddles

the Yangtze River and the Pearl River, with an average temperature of 10 °C to 18 °C, annual precipitation of 1000–1500 mm, a relative humidity of more than 70%, a sunshine duration of 1300 h a year, and a frost-free period of approximately 270 days. It has a rock exposure of 109,000 km^2, accounting for 61.9% of the province's land area. Influenced by climate, soil, and mountainous terrain, vegetation types are diverse in the province. The central, northern and southern parts of the province are dominated by subtropical evergreen broad-leaved forests. The central and eastern parts have tropical moist forests, whereas semi-humid forests are found in the western part of the province. Moreover, cold and warm subalpine coniferous forests cover high-altitudinal areas, while karst evergreen and secondary deciduous broad-leaved mixed forests are found in regions of limestone and dolomite [6,31]. There are 269 families, 1655 genera, and 6255 species of vascular plants (excluding bryophytes) in Guizhou Province. The flora is dominated by tropical and subtropical geographical components (http://lyj.guizhou.gov.cn/, accessed on 20 April 2022). Conifer genera such as Pinus massoniana, Cunninghamia lanceolata, Cupressus, Pinus armandii, and Cryptomeria were the main tree species, and broad-leaved genera included Liquidambar formosana, Quercus glauca, Betula luminifera, Quercus acutissima, Quercus fabri, etc.

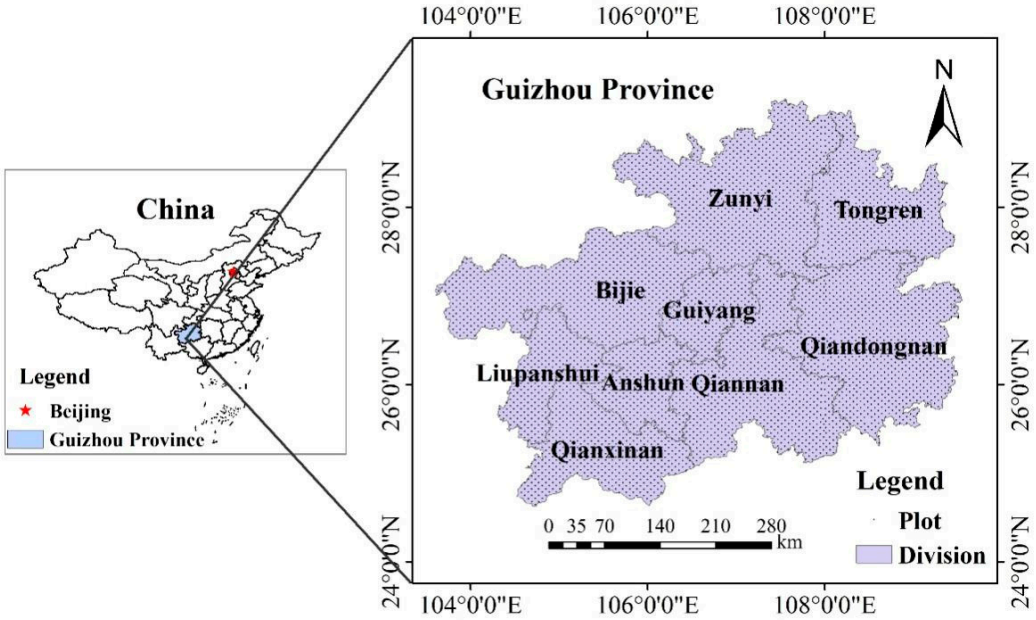

Figure 1. The geographical location of Guizhou province.

2.2. Data Sources

In this study, the seventh NFCI data of the Guizhou province in 2015 were mainly used, which conform to the materials of "The NFCI provision in 2015" and "The NFCI of Guizhou technical regulations". The NFCI data have 5500 fixed plots, arranged according to the topographic map of the whole province, at 4 km high × 8 km wide. Each plot has an area of 0.067 hm^2 (25.82 m × 25.82 m) and is classified as either forest land use or non-forest land use. The biomass equation used in this study was obtained by fitting the model according to the destructive data set (including the total weight of leaves, branches, and roots) in Guizhou province that had been measured in the previous period (Table 1). The biomass equation for tree species in broad-leaved forests was obtained from the study carried out by Zuo et al. [32]. The biomass of bamboo forests was calculated according to the equation developed by Pan et al. [33] for estimating bamboo biomass (Table 1). The sum biomass of each tree in each plot was considered to be the biomass of the plot, and then the biomass density was calculated for each plot. The biomass of shrubs and sparse forests with carbon stocks was 19.76 t·hm^{-2}, while for the economic forests, it was 23.7 t·hm^{-2} [31]. The tree species, without a clear corresponding model, were referred to as

the approximate dominant tree species groups. The biomass of non-forest land trees was calculated as shown in Table 1. The biomass of non-forest lands without standing trees and other forest lands without estimated forest volume had a value of 0. Finally, the total biomass at different regional scales was obtained using the geographical location attribute information of the plots.

Table 1. Fitting equations for aboveground forest biomass of different tree species.

Equation	Tree Species	Fitting Equation	Index
(1)	*Cunninghamia lanceolata*	$y = 0.0687 \cdot DBH^{2.4175}$	$R^2 = 0.9009$
(2)	*Pinus massoniana*	$y = 0.0874 \cdot DBH^{2.4547}$	$R^2 = 0.9103$
(3)	*Pinus yunnanensis*	$y = 0.0794 \cdot DBH^{2.4594}$	$R^2 = 0.9361$
(4)	*Pinus armandii*	$y = 0.1276 \cdot DBH^{2.2911}$	$R^2 = 0.9403$
(5)	*Broad-leaved tree*	$y = 0.1646 \cdot DBH^{2.3916}$	$R^2 = 0.9400$
(6)	*Phyllostachys edulis*	$y = 0.1574 \cdot DBH^{2.3049} + 2.3079$	[33]

y denotes the forest aboveground biomass of different tree species. The biomass of *Cunninghamia lanceolata*, *Abies*, *Tsuga*, *Keteleeria*, *Pseudotsuga*, *Cryptomeria*, *Metasequoia*, *Taxus* and *Cephalotaxus* was calculated by Equation (1). The biomass of coniferous trees such as *Pinus massoniana*, *Pinus thunbergii*, *Pinus kesiya*, *Pinus elliottii*, *Pinus fenzeliana*, *Pinus taiwanensis*, *Cupressus*, *Platycladus*, *Juniperus* and conifer forests was calculated by Equation (2). The biomass of *Pinus armandii*, and *Podocarpus macrophyllus* was calculated by Equation (4). The biomass of other soft broad-leaved and Hardwood tree such as *Lauraceae*, *Quercus* and *Betula* was calculated according to Equation (5).

Forest land plot data were used to explore the biotic and abiotic factors that affect biomass, and all plot data were used to analyze the spatial heterogeneity of forest biomass and explore spatial factors based on the dbMEM method. Forest biomass in this study refers to forest aboveground biomass.

2.3. Analysis of Spatial Heterogeneity of Forest Biomass

The spatial heterogeneity of forest biomass was analyzed using a semi-variance function [34]. In geographical research, the semi-variance function is used as a tool to link the ground model to spatial variation. It can describe the spatial change characteristics of forest biomass by measuring the spatial variation in a regional variable and then establishing the relationship between the ground scene model and the regional variable. Common fitting models include spherical, exponential, linear, and Gaussian. $\gamma(h)$ is defined as the isotropic semi-variance function as follows:

$$\gamma(h) = \frac{1}{2N(h)} \sum_{i=1}^{N(h)} [Z(x_i + h) - 2(x_i)]^2 \quad (7)$$

where $\gamma(h)$ is the semi-variance value of the lag distance (h); $N(h)$ is the number of pairs of data separated by lag distance (h); and $Z(x_i)$ and $Z(x_i + h)$ represent forest biomass values at the coordinates x_i and $(x_i + h)$, respectively.

Anisotropic semivariogram was used to analyze the direct variation in spatial heterogeneity of forest biomass [35]. Generally, anisotropy ratios ($K(h)$) between semivariograms in different directions were used to describe the characteristics of anisotropic structures as follows:

$$K(h) = \gamma(h, \theta_1) / \gamma(h, \theta_2) \quad (8)$$

where $\gamma(h, \theta_1)$ and $\gamma(h,\theta_2)$ are $\gamma(h)$ values in θ_1 and θ_2 directions, respectively. When $K(h)$ equals or is close to 1, the spatial heterogeneity is isotropic; otherwise, it is anisotropic [35].

Moran's I is a commonly used indicator of spatial autocorrelation. In this paper, Global Moran's I was used as the first tool measuring spatial autocorrelation, with values ranging from -1 to 1. The value "1" indicates a perfect positive spatial autocorrelation, while "-1" suggests the perfect negative spatial autocorrelation, and "0" implies perfect spatial randomness [36]. The local Moran's I index was used to indicate whether there was spatial autocorrelation and examine the level of spatial autocorrelation between the characteristic variable (here forest biomass) of each sampling point and its surrounding variables [37],

and it allowed us to identify spatial clusters and spatial outliers of the characteristic variable. A high positive local Moran's *I* value indicates that the target value is similar to its neighborhood, and the locations are spatial clusters, including high–high clusters (high values in a high-value neighborhood) and low–low clusters (low values in a low-value neighborhood). Meanwhile, a high negative local Moran's *I* value implies potential spatial outliers, mainly including high–low (a high value in a low-value neighborhood) and low–high (a low value in a high-value neighborhood) outliers. The formulas and more detailed information on spatial autocorrelation analysis can be found in the literature [36,37].

2.4. Determination of Biotic and Abiotic Factors

To determine the main factors driving the spatial heterogeneity of forest biomass, biotic and abiotic factors were derived from each plot. There were a total of eight biotic factors, including average stand height (m), stand age (average age of dominant tree species in main layer), stand basal area (m^2/ha), stand density (trees/ha), shrub coverage (%), forest categories (protection forest, timber forest, non-timber forest product, firewood forest, special-use forest), stand origin (planted forest, natural forest), and the forest structure of tree species (bamboo forest, coniferous forest, broad-leaved forest, coniferous and broad-leaved mixed forest, shrub meadow, other cultivated plant species). There were a total of 16 abiotic factors, including elevation (m), slope aspect categories (north slope, northeast slope, east slope, southeast slope, south slope, southwest slope, west slope, northwest slope, no slope aspect), slope position categories (ridge, upper slope, middle slope, lower slope, valley, flat), slope (°), soil thickness (<40 cm: thin; 40–80 cm: medium; >80 cm: thick), accessibility (<1 km: acceptable; 1–5 km: accessible; >5 km: to reach), bedrock exposure rate (%), annual mean temperature (°C), annual maximum temperature (°C), annual minimum temperature (°C), annual precipitation (mm), topographic wetness index, canopy density, the thickness of the litter (cm), land types (arbor forest land, bamboo forest land, shrub forest land, cash forest land, other forest land, and unforested land) and humus layer thickness (cm). Among them, the topographic wetness index (TWI) was derived from ASTER GDEM data with 30 m spatial resolution, combined with the coordinates of sampling sites [38]. The annual mean temperature, annual maximum temperature, annual minimum temperature, and annual mean precipitation were obtained based on daily temperature and precipitation data from 19 meteorological stations in Guizhou province in 2015 based on the Kriging interpolation technique with 2 km spatial resolution grid images, combined with various geographical coordinates. Taking into account the influence of humans, accessibility is defined by calculating the minimum distance between the road and the sample using the superposition method to analyze data from the Guizhou province traffic network and the sample coordinates to generate the nearest neighbor table. The mean height of the stand, the density of the stand and the basal area of the stand were calculated on the basis of the plot data. Other factors were determined directly based on the NCFI data.

Furthermore, the distance-based Moran's eigenvector map (dbMEM) was used to analyze spatial changes in forest biomass in Guizhou Province. The dbMEM method, derived from the optimization method developed by Dray et al. [39] using the principal coordinate analysis of neighbor matrices (PCNM), is a sophisticated tool used to model spatial structures [40]. It facilitates the measurement of spatial autocorrelation of feature vectors related to most ecological studies, as it has a stronger ability to analyze spatial scales [40]. The Euclidean distance matrix between plots was calculated according to plot coordinates to generate a truncation matrix. The principal coordinate analysis (PCoA) of the truncated distance matrix was carried out and significant spatial variables were selected by forward selection. Based on the spatial autocorrelation of forest biomass and the intrinsic interrelationship between biotic and abiotic factors, the method of partitioning the variance in multiple regression analysis was used to separate the fractions into a pure fraction and a shared fraction of biotic, abiotic, and spatial factors [41]. Multicollinearity of factors was examined using variance inflation factors (VIF) before using variance partitioning. The

factors for each predictor variable were checked, and if the VIF < 10, multicollinearity was likely not present [42].

2.5. Data Analysis

The Kriging interpolation method was used to interpolate biomass, TWI, and climate factors of the sample plots. The accessibility analysis was carried out using the "Create Near Table" method in ArcGIS (Version 10.6, Esri, Redlands, CA, USA). The software GS+ version 9.0 was used to fit the semivariogram models to analyze the spatial heterogeneity of forest biomass. The Moran's I was calculated using the GeoDa software (Version 1.18, Luc Anselin, Tempe, AZ, USA). The Box–Cox function in the "MASS" package of R (Version 4.1.1, R Development Core Team, Vienna, Austria) [43] was used to transform the data to achieve normality, and the "dbMEM" function in the "Vegan" package was used to calculate the truncation matrix. The forward selection with the "forward.sel" function in the "packfor" package was used to obtain the optimal environmental and spatial structure predictors affecting forest biomass ($p < 0.05$ after 999 simulations) [44]. The "varpart" function in the "vegan" package was used to conduct variance partitioning analysis and calculate the contribution rate of each factor [45].

3. Results

3.1. Spatial Distribution of Forest Biomass

The distribution of forest biomass in Guizhou province showed strong spatial variation, with a CV (coefficient of variation) of 163%. The larger fraction of forest biomass was mainly distributed in the southeast area, the eastern area, and the northwest of Guizhou Province, while the smaller fraction of forest biomass was mainly distributed in western Guizhou Province (Figure 2). Among the semi-variance models (Table 2), the exponential model, which showed a strong spatial autocorrelation of forest biomass within a distance of 15 km, performed the best (R^2 = 0.36). The spatial structural factors accounted for 90% of the spatial heterogeneity of forest biomass, while random factors accounted for 10%. The analysis of the anisotropy ratios of semivariograms showed the 30 km scale changes in forest biomass in all directions. The anisotropy of forest biomass in the northwest–southeast direction ($\theta = 135°$) was the most obvious, followed by that in the east–west direction (0°). The anisotropy of forest biomass in the northeast–southwest (45°) and north–south (90°) directions, however, was relatively low (Figure 3). The distribution of forest biomass in the study area showed positive spatial autocorrelation (Moran's $I = 0.573$, $p < 0.05$). The results of the analysis of Local Moran's I showed that the southeastern part of Guizhou province is identified as an area with high-value spatial clusters, followed by the northwest region, which mainly consists of high–high spatial clusters and low–high spatial outliers (Figure 4).

3.2. Factors Affecting Variation in Forest Biomass

Fourteen factors significantly affected variation in forest biomass (Table 3) after performing forward selection, and collinearity between those factors was low when the VIF was lower than 10. Among the biotic factors, average stand height had the greatest influence on forest biomass, followed by tree species structure, stand basal area, stand origin, shrub cover, stand density, and stand age. Among the abiotic factors, however, annual precipitation had the greatest effect on forest biomass, followed by slope, land type, bedrock exposure rate, canopy cover, the thickness of litter, and elevation.

Table 2. The semivariation model for forest biomass estimation in Guizhou Province.

Model	Nugget (C_0)	Still ($C_0 + C$)	Nugget Coefficient ($C_0/(C_0 + C)$)	Range /km	Residual Sum of Squares (RSS)	R^2
Spherical	0.38	9.49	0.04	17.7	0.371	0.35
Exponential	0.93	9.49	0.10	15.0	0.365	0.36
Linear	9.13	9.76	0.94	297.3	0.05	0.91
Gaussian	1.47	9.48	0.16	14.7	0.371	0.35

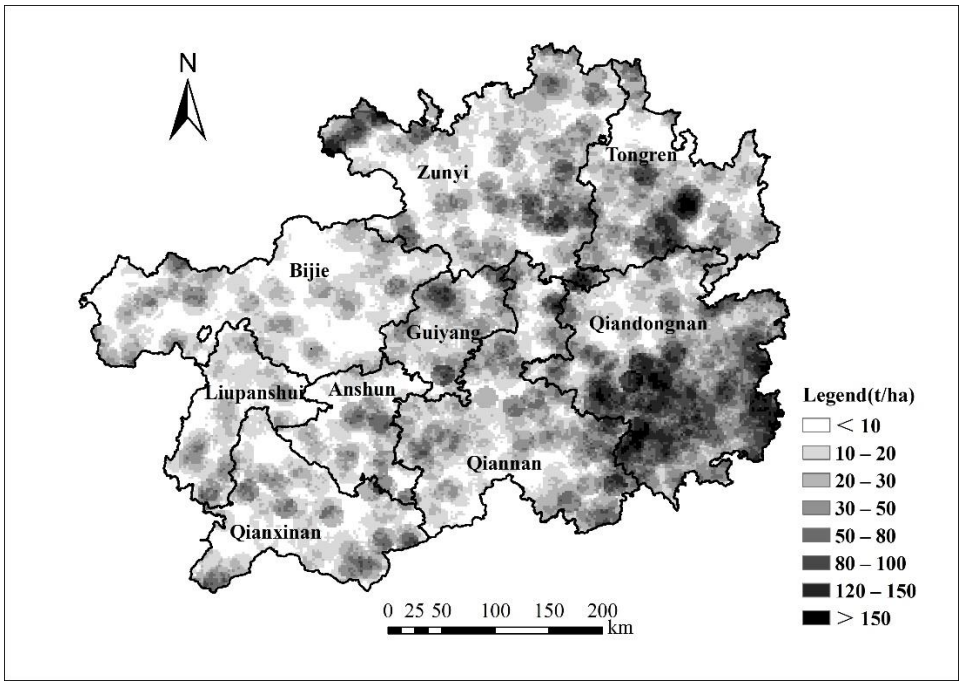

Figure 2. Spatial distribution of forest biomass in Guizhou Province.

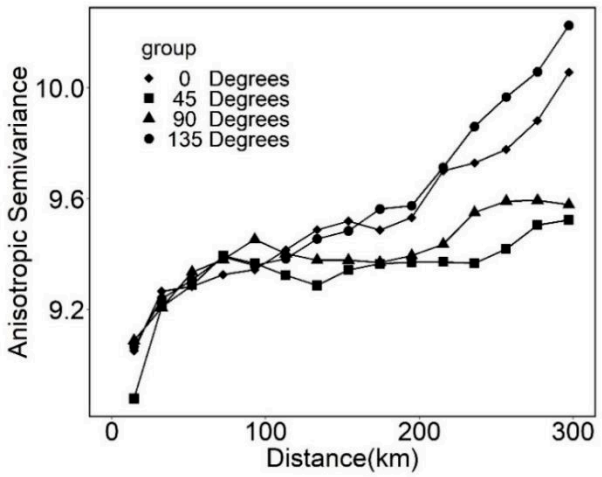

Figure 3. Anisotropic semivariograms for forest biomass in four directions, including east–west (0°), south–north (90°), northeast–southwest (45°), and northwest–southeast (135°) in Guizhou Province.

The results of the variance partition showed that 37% of the total variation in forest biomass was explained by biotic, abiotic, and spatial factors (six dbMEMs) (Figure 5), which explained 34.5%, 19.2%, and 0.7% of the variation, respectively. Pure biotic factors significantly explained 17.4% of the variation ($p < 0.001$), whereas pure abiotic factors significantly explained 2.3% of the variation ($p < 0.001$), and pure spatial factors significantly explained 0.3% of the variation ($p < 0.001$). Biotic and abiotic factors together explained 16.7% of the variation, and biological, abiotic, and spatial factors together explained 0.1% of the variation. The scatterplots demonstrating the relationships between the forest biomass and influencing factors are shown in Figure 6. Biomass increased with increasing stand basal area, annual precipitation, stand density, average stand height, slope, stand age, and canopy density. The biomass decreased with increasing elevation, litter thickness, bedrock exposure rate, and shrub coverage. The biomass per unit area of forest categories was in the order of bamboo forest > arbor forest > cash forest > shrub forest > other forest. The biomass per unit area of natural forest had a higher value than that of planted forest.

For the tree species structure, the biomass per unit area was in the order of broad-leaved mixed forest > coniferous, mixed forest > coniferous forest > coniferous and broad-leaved mixed forest > broad-leaved forest (Figure 7). In addition, in the eastern (Qiandongnan and Qiannan) and northwestern (Zunyi) regions, the soil thickness is higher than that in other regions, and the exposure rate of bedrock is also significantly lower than that in other regions (Table 4). Six spatial vectors in 2733 dbMEMs were significant, and the 25th, 32th, and 90-dbMEM were large-scale vectors, while the 143rd, 147th, and 425-dbMEM were medium-scale vectors (Figure 8).

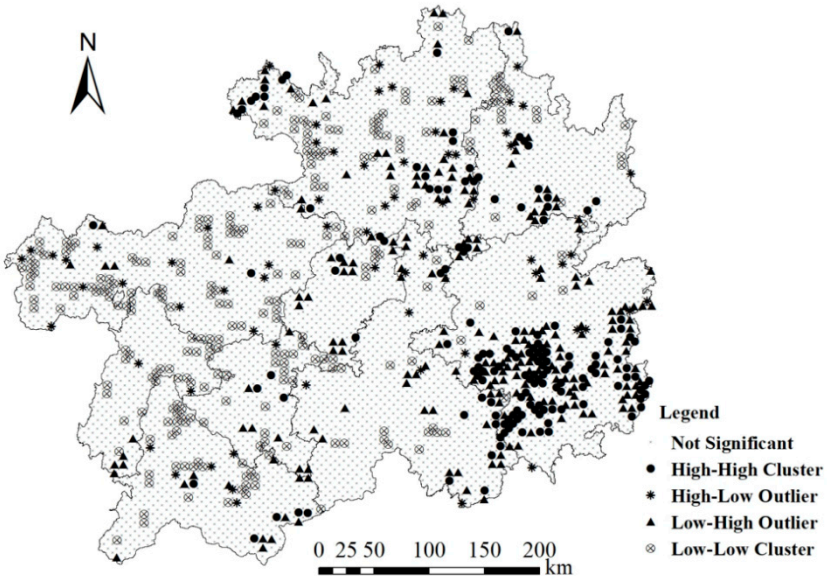

Figure 4. Maps of the Local Moran's Index of forest biomass in Guizhou Province.

Table 3. Factors and parameters obtained after performing forward selection.

Factors	Adjusted R^2	F	*p*-Value	VIF
Average stand height	0.184	1245.08	0.001	6.73
Tree species structure	0.078	580.69	0.001	2.63
Stand basal area	0.033	261.95	0.001	5.15
Stand origin	0.028	226.75	0.001	2.6
Shrub coverage	0.009	78.94	0.001	2.07
stand density	0.008	69.67	0.001	4.78
Annual precipitation	0.007	59.81	0.001	1.08
Slope	0.005	41.17	0.001	1.46
Land type	0.003	30.83	0.001	3.32
Exposure rate of bedrock	0.003	27.2	0.001	1.23
Canopy density	0.003	23.93	0.001	7.72
Thickness of litter	0.002	19.11	0.001	2.09
Stand age	0.001	13.18	0.001	3.1
Elevation	0.001	12.2	0.001	1.1

Table 4. Soil thickness and bedrock exposure rate in various cities of Guizhou Province.

	Category	Anshun	Bijie	Guiyang	Liupanshui	Qiandongnan	Qiannan	Qianxinan	Tongren	Zunyi	Number of Spots
Soil thickness	Thin	227	640	187	245	419	519	360	344	631	3572
	Medium	31	120	33	26	157	172	104	137	212	992
	Thick	22	80	41	33	369	124	65	87	115	936
Exposure Rate of bedrock (%)	≤10	270	810	257	301	207	791	495	545	930	4606
	(10,50]	9	30	3	3	585	22	33	23	21	729
	>50	1	0	1	0	153	2	1	0	7	165
Number of spots	—	280	840	261	304	945	815	529	568	958	5500

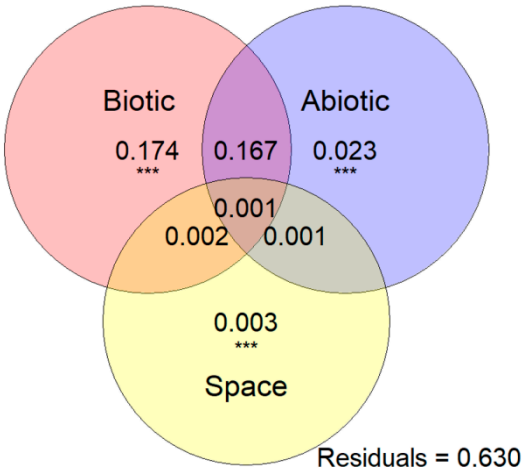

Figure 5. Variance partitioning results for forest biomass among biotic, abiotic, and spatial factors; *** indicates $p < 0.001$.

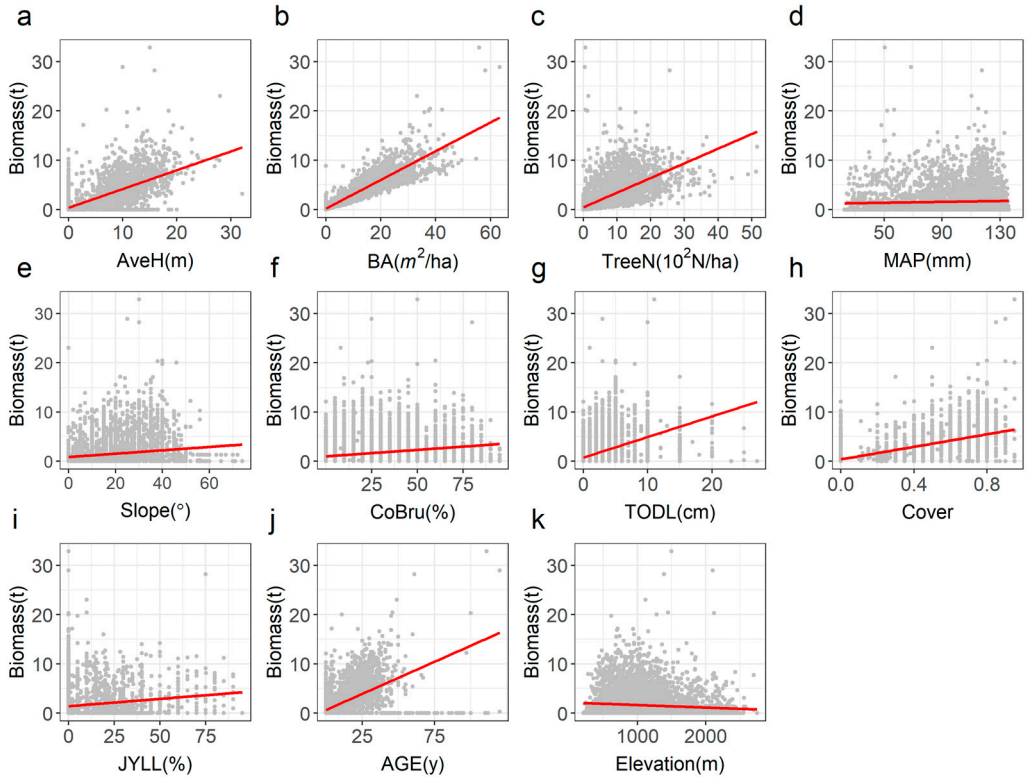

Figure 6. Scatterplots demonstrating the relationships between forest biomass and five biotic factors and six abiotic factors; (**a**) AveH, average stand height; (**b**) BA, stand basal area; (**c**) TreeN, stand density; (**d**) MAP, annual precipitation; (**e**) Slope, slope; (**f**) CoBru, shrub coverage; (**g**) TODL, the thickness of litter; (**h**) Cover, canopy density; (**i**) JYLL, bedrock exposure rate; (**j**) AGE, stand age; (**k**) Elevation.

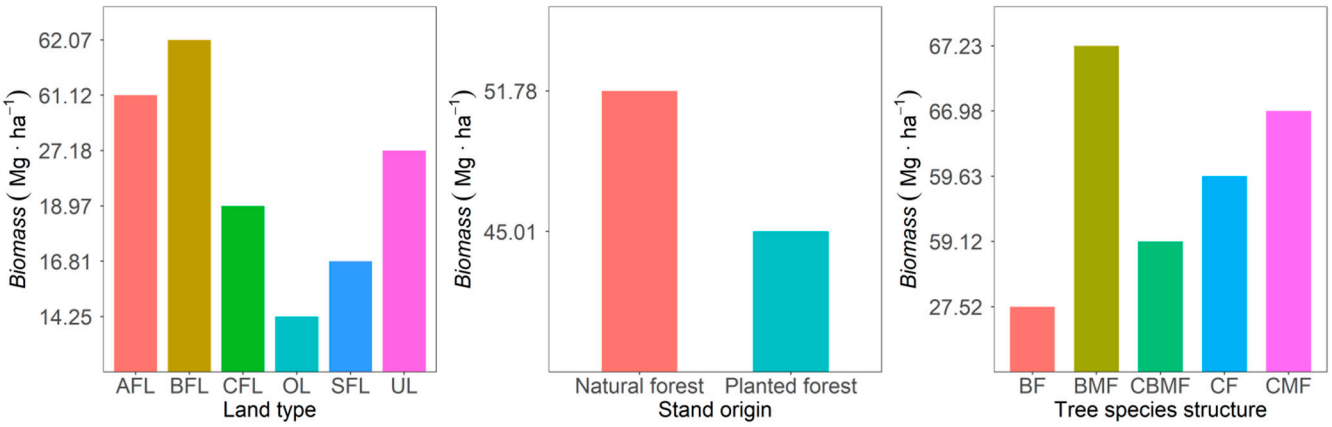

Figure 7. Relationships between forest biomass and land type, stand origin, and tree species structure. Land type: AFL; arbor forest land, BFL; bamboo forest land, SFL; shrub forest land, CFL; cash forest land, OL; other forest land, UL; unforested land. Tree species structure: CF; coniferous forest, BF; broad-leaved forest, CMF; coniferous mixed forest, CBMF; coniferous and broad-leaved mixed forest, BMF; broad-leaved mixed forest.

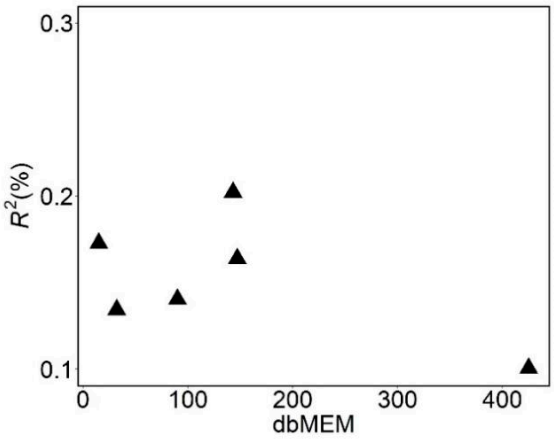

Figure 8. The variation (%) in biomass explained by dbMEM eigenvectors obtained after performing the forward selection procedure and controlling the stand and topographic variables.

4. Discussion

4.1. Biotic Factors

There was a strong spatial heterogeneity in the forest biomass in Guizhou Province. The results of the variance partitioning analysis showed that 34.4% of the spatial variation in forest biomass in Guizhou province was explained by biotic factors (Figure 5). The larger the basal area, average stand height, stand age, and stand density, the higher the aboveground biomass and shrub coverage and the lower the forest biomass (Figure 6). Many studies have confirmed that the stand basal area and stand height are the main predictors of forest biomass [15,46,47], as they influence biomass by affecting the unit trunk volume. Some studies have even shown that the forest stand biomass can be estimated to a certain extent by estimating the biomass of large trees [12]. With the forest growth, the rate of biomass accumulation in trunks was higher than that in branches and leaves [48]. Compared with young forests, mature forests have more complex development stages [3], faster root-specific metabolisms, higher nutrient absorption [25], and a greater capacity for accumulation capacity [13,14,49,50]. With increasing stand density, trees occupy more space and utilize more energy, light, water, and soil nutrients [16], which is conducive to increasing individual complementarity [51] and improving forest biomass [52]. The shrub is in the lower layer of vegetation in the forest, which overlaps the ecological niche of the canopy tree species, and they both compete for light, soil nutrients, and water

resources [53,54]; therefore, the shrub coverage for stands with high forest biomass is usually lower. Furthermore, the biomass per unit of area of the mixed forest was higher than that of the pure forest, and that of the coniferous forest was higher than that of the broad-leaved forest (Figure 7). On the one hand, when compared with that of the pure forest, the structure of the mixed forest stand was complex and could better resist natural disturbances, such as pests and diseases [55]. On the other hand, the species richness of the mixed forest was higher than that of the pure forest, which supported the effect of niche complementarity to some extent [19]. Compared to broad-leaved trees, conifers have smaller percentages of mass of branches and leaves, and more biomass is allocated in conifers to the trunk, making the biomass of conifers high [56]. Our results provide an important reference for future local afforestation plans and management measures. Targeted planting (such as the planting of conifers) can better store forest carbon and mitigate the adverse effects of greenhouse gases [2,57].

4.2. Abiotic Factors

In our study, the average rate of the contribution of abiotic factors to the spatial heterogeneity of forest biomass was 19.2% (Figure 5). Forest biomass was negatively correlated with elevation but positively correlated with annual precipitation, slope, canopy density, and bedrock exposure rate (Figure 6). The terrain of Guizhou province is high in the west and low in the east, and the distribution patterns of forest biomass showed a trend of increasing from west to east (Figure 2). Compared with high-altitude areas, low-altitude areas often have high temperatures [58], which allows for an increased supply of nitrogen and phosphorus to plant leaves [59], thus improving the photosynthesis of plants and promoting the growth of forest trees. Trees at high altitudes tend to grow to shorter heights [59]. Therefore, forest biomass generally decreases along the elevation gradient [6,60,61]; however, this can be affected by other factors such as logging [48]. Moreover, elevation can also affect forest biomass by influencing rainfall and controlling soil moisture conditions [13,62]. Numerous studies have demonstrated that forest biomass decreases with the increase of slope [27,63], which is in contradiction to our results. In general, trees struggle to grow in a forest with a high slope [27], and vegetation often grows more luxuriantly and has higher biomass in a region with a low slope [63]. However, most areas in Guizhou province with low slopes are designated as agricultural lands with few trees, while afforestation is carried out in lands that have high slopes or are unsuitable for farming [6]. In addition, due to the occurrence of typical karst landforms in Guizhou Province, most tree species tend to grow on slopes and hilltops [64], which allows for higher forest biomass production in areas with higher slopes. Precipitation can regulate water distribution and affect water availability [21]. Studies have shown that biomass production in subtropical and tropical forests is mainly restricted by water [15]. Generally, canopy density is determined by the species composition and stand attributes of trees (DBH, tree height) [13]. The better the growth, the higher the canopy density. At the same time, canopy closure maximizes light interception at the stand level [65] and also rainfall interception and redistribution [66], promotes the efficient heat and water exchange between the surface and atmosphere, and regulates forest microclimatic conditions (e.g., surface temperature). Thus, the net available energy of vegetation increases, and forest productivity is also affected [67]. Karst landforms in Guizhou province are distributed in large areas, with serious soil erosion and rocky desertification [31]. Areas with high bedrock exposure rates have shallow soil layers, which generally do not contribute to forest growth. Figures 2 and 3 show that larger fractions of forest biomass are distributed in southeast, northwest, and eastern Guizhou province. Forest biomass exhibited a gradually decreasing trend from east to west, which is also related to the greater thickness of the soil layer and the lower rate of surface bedrock exposure in eastern and northwestern regions (Table 4), which surround the Yangtze River and the Pearl River, with excellent geographical conditions and considerable vegetation growth, while in other regions, the vegetation growth is poor due to poor water quality [68]. Among the vegetation types, the bamboo forest had the highest biomass per unit area,

because bamboo grows in branching clusters and also has a higher plant density level per unit area [31,33]. Furthermore, bamboo forests are distributed mainly in the Chishui River basin in the northwest of Guizhou and the Qingshui River basin in the eastern part of Guizhou. However, arbor forests are distributed throughout the province, with lower biomass per unit area than bamboo forests. Since 2000, forestry activities implemented in Guizhou province, such as mountain closure, cultivating the forests, and reducing man-made damage to natural forests, may be the main reason that the biomass per unit area of natural forests is generally higher than that of planted forests. Due to the small latitude difference in Guizhou Province, the climate factors did not reflect the contribution to forest biomass in this study, but the complex and diverse terrain conditions formed a diversified microclimate environment, indirectly affecting forest biomass. Studies have shown that the global annual average surface temperature and precipitation are currently increasing at a rate of 0.19 °C and 2.04 mm per decade between 1901 and 2015 [57]. Combined with the results (Figure 6d), we suggested in the restoration of afforestation and vegetation that the effects of precipitation, topographic factors, and bare rock leakage should be considered to cope with climate change in the coming period.

4.3. Spatial Factors and Their Interactions

The results showed that there was a strong spatial autocorrelation of forest biomass distribution in Guizhou province (Figure 3). Variance partitioning results revealed that spatial factors influenced forest biomass at the broad and meso scales (Figure 8) but explained only 0.7% of the variation in total forest biomass (Figure 5). On the one hand, the spatial autocorrelation of forest biomass is driven by the abiotic factors which were measured in our study and spatially autocorrelated. Many studies have reported that precipitation, elevation, slope, and land-use type showed a certain extent of spatial autocorrelation [40,69]. In our study, significant factors affecting forest biomass distribution could explain the spatial autocorrelation to some extent. However, we cannot rule out the possibility that the forest biomass obtained is strongly influenced by other predictors not included in this study, such as environmental data (e.g., soil nutrients). In the large study area, some data are difficult to obtain, and it is also costly to perform a field investigation. Furthermore, though random (stochastic) processes only account for 10% of the variation in forest characteristics (Table 2), they may still exert an important influence. On a large scale, stochastic processes are often related to deterministic processes, while on a small scale, deterministic processes tend to dominate [70]. Additionally, biotic and abiotic factors together explained 16.7% of the total variation, while biotic, abiotic, and spatial factors together only explained 0.1% of the variation. Zhang et al. [20] showed a strong interaction between stand age and other climatic factors, such as precipitation, that caused changes in forest biomass. Luo et al. [71] reported that the forest biomass was related to the interaction between climatic factors (annual precipitation and annual mean temperature) and stand density. Therefore, the growth and distribution of vegetation are the results of a combination of multiple factors.

5. Conclusions

We analyzed the spatial heterogeneity of forest biomass and its main influencing factors in Guizhou province using the NFCI data from 5500 fixed sample plots in 2015. The forest biomass in Guizhou had a strong spatial heterogeneity. The areas with large stocks of forest biomass are mainly distributed in the southeast and northwest of Guizhou, while forests with low biomass are mainly distributed in the west of Guizhou. Stand characteristics such as average stand height, tree species structure, stand basal area, origin, shrub coverage, stand density, and stand age, abiotic factors, including annual precipitation, slope, land type, basalt rock exposure, canopy density, litter thickness, and altitude, and spatial factor (spatial autocorrelation) explained 37% of the total variance in forest biomass in Guizhou province. Among them, biotic factors explained the most variation, followed by abiotic factors and spatial factor, which explained a slight variation (0.7%). This study quantified the factors that control the spatial heterogeneity of forest biomass, which can help

to deepen the understanding of carbon sequestration and provide a basis for formulating more effective forest management strategies in subtropical karst forests.

Author Contributions: Conceptualization, T.Z. and Y.Q.; methodology, T.Z.; software, T.Z.; validation, Y.Q., G.D. and J.Z.; formal analysis, T.Z.; investigation, J.Z.; resources, G.D. and J.Z.; data curation, T.Z.; writing—original draft preparation, T.Z.; writing—review and editing, T.Z. and Y.Q.; visualization, T.Z.; supervision, Y.Q.; project administration, G.D. and J.Z.; funding acquisition, Y.Q. All authors have read and agreed to the published version of the manuscript.

Funding: This research was funded by the National Key Research and Development Program of China, grant number 2017YFD06003002; the National Natural Science Foundation of China, grant number 32060266; Guizhou Province science and Technology plan project (post-subsidy plan project), grant number QKHPTRC [2018]5261.

Institutional Review Board Statement: Not applicable.

Informed Consent Statement: Not applicable.

Data Availability Statement: Data are available upon request from the corresponding author.

Conflicts of Interest: The authors declare no conflict of interest.

References

1. Liu, G.H.; Fu, B.J.; Fang, J.Y. Carbon dynamics of Chinese forests and its contribution to global carbon balance. *Acta Ecol. Sin.* **2000**, *20*, 732–740.
2. Tang, X.L.; Zhao, X.; Bai, Y.F.; Tang, Z.Y.; Wang, W.T.; Zhao, Y.C.; Wan, H.W.; Xie, Z.Q.; Shi, X.Z.; Wu, B.F.; et al. Carbon pools in China's terrestrial ecosystems: New estimates based on an intensive field survey. *Proc. Natl. Acad. Sci. USA* **2018**, *115*, 4021–4026. [CrossRef] [PubMed]
3. Zald, H.S.J.; Spies, T.A.; Seidl, R.; Pabst, R.J.; Olsen, K.A.; Steel, E.A. Complex mountain terrain and disturbance history drive variation in forest aboveground live carbon density in the western Oregon cascades, USA. *For. Ecol. Manag.* **2016**, *366*, 193–207. [CrossRef] [PubMed]
4. Tarun, K.T.; Swamy, S.L.; Arvind, B.; Mammohan, J.R.D. Assessment of biomass and net primary productivity of a dry tropical forest using geospatial technology. *J. For. Res.* **2019**, *30*, 157–170. [CrossRef]
5. Nicolas, P.; Gamarra, J.G.P.; Luca, B.; Anne, B. Plot-level variability in biomass for tropical forest inventory designs. *For. Ecol. Manag.* **2018**, *430*, 10–20. [CrossRef]
6. Qian, C.H.; Qiang, H.Q.; Zhang, G.M.; Li, M.Y. Long-term changes of forest biomass and its driving factors in karst area, Guizhou, China. *Int. J. Distrib. Sens. Netw.* **2021**, *17*. [CrossRef]
7. Fang, J.Y.; Chen, A.P.; Peng, C.H.; Zhao, S.Q. Changes in forest biomass carbon storage in China between 1949 and 1998. *Science* **2001**, *292*, 2320–2322. [CrossRef]
8. Magnussen, S.; Nord-Larsen, T.; Riis-Nielsen, T. Lidar supported estimators of wood volume and aboveground biomass from the danish national forest inventory (2012–2016). *Remote Sens. Environ.* **2018**, *211*, 146–153. [CrossRef]
9. Huang, H.B.; Liu, C.X.; Wang, X.Y.; Zhou, X.L.; Gong, P. Integration of multi-resource remotely sensed data and allometric models for forest aboveground biomass estimation in China. *Remote Sens. Environ.* **2019**, *221*, 225–234. [CrossRef]
10. Kim, T.J.; Bullock, B.P.; Stape, J.L. Effects of silvicultural treatments on temporal variations of spatial autocorrelation in Eucalyptus plantations in Brazil. *For. Ecol. Manag.* **2015**, *358*, 90–97. [CrossRef]
11. Lin, Z.; Chao, L.; Wu, C.; Hong, W.; Hong, T.; Hu, X. Spatial analysis of carbon storage density of mid-subtropical forests using geostatistics: A case study in Jiangle County, southeast China. *Acta Geochim.* **2017**, *37*, 90–101. [CrossRef]
12. Xu, L.; Shi, Y.; Fang, H.; Zhou, G.; Xu, X.; Zhou, Y.; Tao, J.; Ji, B.; Xu, J.; Li, C.; et al. Vegetation carbon stocks driven by canopy density and forest age in subtropical forest ecosystems. *Sci. Total Environ.* **2018**, *631–632*, 619–626. [CrossRef] [PubMed]
13. Xu, Y.Z.; Franklin, S.B.; Wang, Q.G.; Shi, Z.; Luo, Y.Q.; Lu, Z.J.; Zhang, J.X.; Qiao, X.J.; Jiang, M.X. Topographic and biotic factors determine forest biomass spatial distribution in a subtropical mountain moist forest. *For. Ecol. Manag.* **2015**, *357*, 95–103. [CrossRef]
14. Liu, Y.C.; Yu, G.R.; Wang, Q.F.; Zhang, Y.J. How temperature, precipitation and stand age control the biomass carbon density of global mature forests. *Glob. Ecol. Biogeogr.* **2014**, *23*, 323–333. [CrossRef]
15. Ouyang, S.; Xiang, W.H.; Wang, X.P.; Xiao, W.F.; Chen, L.; Li, S.G.; Sun, H.; Deng, X.W.; Forrester, D.I.; Zeng, L.X.; et al. Effects of stand age, richness and density on productivity in subtropical forests in China. *J. Ecol.* **2019**, *107*, 2266–2277. [CrossRef]
16. Ali, A.; Mattsson, E.; Nissanka, S.P. Big-sized trees and species-functional diversity pathways mediate divergent impacts of environmental factors on individual biomass variability in SriLankan tropical forests. *J. Environ. Manag.* **2022**, *315*, 115177. [CrossRef]
17. Lutz, J.A.; Furniss, T.J.; Johnson, D.J.; Davies, S.J.; Allen, D.; Alonso, A.; Anderson-Teixeira, K.J.; Andrade, A.; Baltzer, J.; Becker, K.M.L.; et al. Global importance of large-diameter trees. *Glob. Ecol. Biogeogr.* **2018**, *27*, 849–864. [CrossRef]

18. Poorter, L.; van der Sande, M.T.; Arets, E.J.M.M.; Ascarrunz, N.; Enquist, B.J.; Finegan, B.; Licona, J.C.; Martínez-Ramos, M.; Mazzei, L.; Meave, J.A.; et al. Biodiversity and climate determine the functioning of Neotropical forests. *Glob. Ecol. Biogeogr.* **2017**, *26*, 1423–1434. [CrossRef]
19. Feng, Y.H.; Schmid, B.; Loreau, M.; Forrester, D.I.; Fei, S.L.; Zhu, J.X.; Tang, Z.Y.; Zhu, J.L.; Hong, P.B.; Ji, C.J.; et al. Multispecies forest plantations outyield monocultures across a broad range of conditions. *Science* **2022**, *376*, 865–868. [CrossRef]
20. Zhang, H.; Song, T.Q.; Wang, K.L.; Yang, H.; Yue, Y.M.; Zeng, Z.X.; Peng, W.X.; Zeng, F.P. Influences of stand characteristics and environmental factors on forest biomass and root–shoot allocation in southwest China. *Ecol. Eng.* **2016**, *91*, 7–15. [CrossRef]
21. Ferry, B.; Morneau, F.; Bontemps, J.D.; Blanc, L.; Freycon, V. Higher treefall rates on slopes and waterlogged soils result in lower stand biomass and productivity in a tropical rain forest. *J. Ecol.* **2010**, *98*, 106–116. [CrossRef]
22. Fisk, M.; Schmidt, S.; Seastedt, T.R. Topographic patterns of above- and belowground production and nitrogen cycling in alpine tundra. *Ecology* **1998**, *79*, 2253–2266. [CrossRef]
23. Zhang, Y.; Chen, H.Y. Individual size inequality links forest diversity and above-ground biomass. *J. Ecol.* **2015**, *103*, 1245–1252. [CrossRef]
24. Conti, G.; Pérez-Harguindeguy, N.; Quètier, F.; Gorné, L.D.; Jaureguiberry, P.; Bertone, G.A.; Enrico, L.; Cuchietti, A.; Díaz, S. Large changes in carbon storage under different land-use regimes in subtropical seasonally dry forests of southern South America. *Agric. Ecosyst. Environ.* **2014**, *197*, 68–76. [CrossRef]
25. McEwan, R.W.; Lin, Y.C.; Sun, I.F.; Hsieh, C.F.; Su, S.H.; Chang, L.W.; Michael Song, G.Z.; Wang, H.H.; Hwong, J.L.; Lin, K.C.; et al. Topographic and biotic regulation of aboveground carbon storage in subtropical broad-leaved forests of Taiwan. *For. Ecol. Manag.* **2011**, *262*, 1817–1825. [CrossRef]
26. Goulden, M.L.; McMillan, A.M.S.; Winston, G.C.; Rocha, A.V.; Manies, K.L.; Harden, J.W.; Bond-Lamberty, B.P. Patterns of NPP, GPP, respiration, and NEP during boreal forest succession. *Glob. Chang. Biol.* **2011**, *17*, 855–871. [CrossRef]
27. Seidl, R.; Schelhaas, M.J.; Rammer, W.; Verkerk, P.J. Increasing forest disturbances in Europe and their impact on carbon storage. *Nat. Clim. Change* **2014**, *4*, 806–810. [CrossRef]
28. Liu, C.; Li, F.R.; Zhen, Z. Prediction of spatial distribution of forest carbon storage in Heilongjiang Province using spatial error model. Chin. *J. Appl. Ecol.* **2014**, *25*, 2779–2786. [CrossRef]
29. Nettesheim, F.C.; Garbin, M.L.; Pereira, M.G.; Araujo, D.S.D.; Grelle, C.E.V. Local-scale elevation patterns of Atlantic Forest tree community variation and assembly drivers in a conservation hotspot in southeastern Brazil. *Flora* **2018**, *248*, 61–69. [CrossRef]
30. Song, L.Y.; Li, M.Y.; Xu, H.; Guo, Y.; Wang, Z.; Li, Y.C.; Wu, X.J.; Feng, L.C.; Chen, J.; Lu, X.; et al. Spatiotemporal variation and driving factors of vegetation net primary productivity in a typical karst area in China from 2000 to 2010. *Ecol. Indic.* **2021**, *132*, 108280. [CrossRef]
31. Tian, X.L.; Xia, J.; Xia, H.B.; Ni, J. Forest biomass and its spatial pattern in Guizhou province. *Chin. J. Appl. Ecol.* **2011**, *22*, 287–294. [CrossRef]
32. Zuo, S.D.; Ren, Y.; Weng, X.; Ding, H.F.; Luo, Y.J. Biomass allometric equations of nine common tree species in an evergreen broadleaved forest of subtropical China. *Chin. J. Appl. Ecol.* **2015**, *26*, 356–362. [CrossRef]
33. Pan, C.X.; Li, X.T.; Lv, U.L. Resources and Biomass of Phyllostachys heterocycla cv. pubescens in Anji. *J. Zhejiang For. Sci. Technol.* **2010**, *30*, 82–84. [CrossRef]
34. Rossi, R.E.; Mulla, D.J.; Journel, A.G.; Franz, E.H. Geostatistical tools for modeling and interpreting ecological spatial dependence. *Ecol. Monogr.* **1992**, *62*, 277–314. [CrossRef]
35. Li, H.B.; Wang, Z.Q.; Wang, Q.C. Theory and methodology of spatial heterogeneity quantification. *Chin. J. Appl. Ecol.* **1998**, *9*, 651–657. [CrossRef]
36. Moran, P.A. Notes on continuous stochastic phenomena. *Biometrika* **1950**, *37*, 17. [CrossRef]
37. Anselin, L. Local indicators of spatial association-LISA. *Geogr. Anal.* **1995**, *27*, 93–115. [CrossRef]
38. Ambroise, B.; Beven, K.; Freer, J. Toward a Generalization of the TOPMODEL Concepts: Topographic Indices of Hydrological Similarity. *Water Resour. Res.* **1996**, *32*, 2135–2145. [CrossRef]
39. Dray, S.; Legendre, P.; Peres-Neto, P.R. Spatial modelling: A comprehensive framework for principal coordinate analysis of neighbour matrices (PCNM). *Ecol. Model.* **2006**, *196*, 483–493. [CrossRef]
40. Legendre, P.; Legendre, L.F. *Numerical Ecology*; Elsevier: Oxford, UK, 2012.
41. Borcard, D.; Legendre, P.; Drapeau, P. Partialling out the spatial component of ecological variation. *Ecology* **1992**, *73*, 1045–1055. [CrossRef]
42. Graham, M.H. Confronting multicollinearity in ecological multiple regression. *Ecology* **2003**, *84*, 2809–2815. [CrossRef]
43. R Development Core Team. *R Version 4.1.1*; R Foundation for Statistical Computing: Vienna, Austria, 2021.
44. Dray, S.; Bauman, D.; Blanchet, G.; Borcard, D.; Clappe, S.; Guenard, G.; Jombart, T.; Larocque, G.; Legendre, P.; Madi, N. Adespatial: Multivariate multiscale spatial analysis. *R Package Version* **2017**, *82*, 3–7. [CrossRef]
45. Oksanen, J.; Kindt, R.; Legendre, P.; O'Hara, B.; Stevens, M.H.H.; Oksanen, M.J. Suggests MASS. The vegan package. *Community Ecol. Package* **2007**, *10*, 719.
46. Stephenson, N.L.; Das, A.J.; Condit, R.; Russo, S.E.; Baker, P.J.; Beckman, N.G.; Coomes, D.A.; Lines, E.R.; Morris, W.K.; Rüger, N.; et al. Rate of tree carbon accumulation increases continuously with tree size. *Nature* **2014**, *507*, 90. [CrossRef] [PubMed]
47. Ali, A.; Chen, H.Y.H.; You, W.H.; Yan, E.R. Multiple abiotic and biotic drivers of aboveground biomass shift with forest Stratum. *For. Ecol. Manag.* **2019**, *436*, 1–10. [CrossRef]

48. Peichl, M.; Arain, M.A. Allometry and partitioning of above- and belowground tree biomass in an age-sequence of white pine forests. *For. Ecol. Manag.* **2007**, *253*, 68–80. [CrossRef]
49. Hui, D.F.; Wang, J.; Shen, W.J.; Le, X.; Ganter, P.; Ren, H. Near Isometric Biomass Partitioning in Forest Ecosystems of China. *PLoS ONE.* **2014**, *9*, e86550. [CrossRef]
50. Dyderski, M.K.; Pawlik, U. Drivers of forest aboveground biomass and its increments in the Tatra Mountains after 15 years. *Catena* **2021**, *205*, 105468. [CrossRef]
51. Ni, Y.Y.; Jian, Z.J.; Zeng, L.X.; Liu, J.F.; Lei, L.; Zhu, J.H.; Xu, J.; Xiao, W.F. Climate, soil nutrients, and stand characteristics jointly determine large-scale patterns of biomass growth rates and allocation in Pinus massoniana plantations. *For. Ecol. Manag.* **2022**, *504*, 119839. [CrossRef]
52. Wang, Y.; Wang, Q.; Wang, M. Similar carbon density of natural and planted forests in the Lüliang Mountains, China. *Ann. For. Sci.* **2018**, *75*, 87. [CrossRef]
53. Zhang, Y.; Chen, H.Y.H.; Taylor, A.R. Positive species diversity and above-ground biomass relationships are ubiquitous across forest strata despite interference from overstorey trees. *Funct. Ecol.* **2017**, *31*, 419–426. [CrossRef]
54. Landuyt, D.; Maes, S.L.; Depauw, L.; Ampoorter, E.; Blondeel, H.; Perring, M.P.; Brumelis, G.; Brunet, J.; Decocq, G.; den Ouden, J.; et al. Drivers of aboveground understorey biomass and nutrient stocks in temperate deciduous forests. *J. Ecol.* **2019**, *108*, 982–997. [CrossRef]
55. Griess, V.C.; Acevado, R.; Hartl, F.; Staupendahl, K.; Knoke, T. Does mixing tree species enhance stand resistance against natural hazards? A case study for spruce. *For. Ecol. Manag.* **2012**, *267*, 284–296. [CrossRef]
56. Poorter, H.; Jagodzinski, A.M.; Ruiz-Peinado, R.; Kuyah, S.; Luo, Y.; Oleksyn, J.; Usoltsev, V.A.; Buckley, T.N.; Reich, P.B.; Sack, L. How does biomass distribution change with size and differ among species? An analysis for 1200 plant species from five continents. *New. Phytol.* **2015**, *208*, 736–749. [CrossRef]
57. Blunden, J.; Arndt, D.S. State of the Climate in 2015. *Bull. Am. Meteorol. Soc.* **2016**, *97*, S1–S275. [CrossRef]
58. Wang, G.; Guan, D.S.; Xiao, L.; Peart, M.R. Forest biomass-carbon variation affected by the climatic and topographic factors in Pearl River Delta, South China. *J. Environ. Manag.* **2019**, *232*, 781–788. [CrossRef]
59. Malhi, Y.; Girardin, C.A.J.; Goldsmith, G.R.; Doughty, C.E.; Salinas, N.; Metcalfe, D.B.; Huasco, W.H.; Silva-Espejo, J.E.; Aguilla-Pasquell, J.D.; Amézquita, F.F.; et al. The variation of productivity and its allocation along a tropical elevation gradient: A whole carbon budget perspective. *New Phytol.* **2017**, *214*, 1019–1032. [CrossRef]
60. Girardin, C.A.J.; Malhi, Y.; Aragão, L.E.O.C.; Mamani, M.; Huasco, H.W.; Durand, L.; Feeley, K.J.; Rapp, J.; Silva-Espejo, J.E.; Silman, M.R.; et al. Net primary productivity allocation and cycling of carbon along a tropical forest elevational transect in the Peruvian Andes. *Glob. Chang. Biol.* **2010**, *16*, 3176–3192. [CrossRef]
61. Sandoya, V.; Saura-Mas, S.; Cerda, G.D.L.; Arellano, G.; Macía, M.J.; Tello, J.S.; Lloret, F. Contribution of species abundance and frequency to aboveground forest biomass along an Andean elevation gradient. *For. Ecol. Manag.* **2021**, *479*, 118549. [CrossRef]
62. Yuan, Z.Q.; Ali, A.; Sanaei, A.; Ruiz-Benito, P.; Jucker, T.; Fang, L.; Bai, E.; Ye, J.; Lin, F.; Fang, S.; et al. Few large trees, rather than plant diversity and composition, drive the above-ground biomass stock and dynamics of temperate forests in northeast China. *For. Ecol. Manag.* **2021**, *481*, 118698. [CrossRef]
63. Wang, X.L.; Yu, C.; Chen, H.W.; Hu, Y.M.; Jiao, L.L.; Feng, Y.T.; Wu, W.; Wu, H.F. Spatial pattern of forest biomass and its influencing factors in the Great Xing'an Mountains, Heilongjiang Province, China. *Chin. J. Appl. Ecol.* **2014**, *25*, 974–982. [CrossRef]
64. Du, H.; Hu, F.; Zeng, F.P.; Wang, K.L.; Peng, W.X.; Zhang, H.; Zeng, Z.X.; Zhang, F.; Song, T.Q. Spatial distribution of tree species in evergreen-deciduous broadleaf karst forests in southwest China. *Sci. Rep.* **2017**, *7*, e15664. [CrossRef] [PubMed]
65. Binkley, D.; Campoe, O.C.; Gspaltl, M.; Forrester, D.I. Light absorption and use efficiency in forests: Why patterns differ for trees and stands. *For. Ecol. Manag.* **2013**, *288*, 5–13. [CrossRef]
66. Sanaei, A.; Chahouki, M.A.Z.; Ali, A.; Jafari, M.; Azarnivand, H. Abiotic and biotic drivers of aboveground biomass in semi-steppe rangelands. *Sci. Total Environ.* **2018**, *615*, 895–905. [CrossRef] [PubMed]
67. Jucker, T.; Bouriaud, O.; Coomes, D.A. Crown plasticity enables trees to optimize canopy packing in mixed-species forests. *Funct. Ecol.* **2015**, *29*, 1078–1086. [CrossRef]
68. Wang, Z.Q.; Liu, B.Y.; Hai, C.X. Effects of soil depth on vegetation cover and above ground biomass in east part of inner Mongolia. *J. Soil Water Consery.* **2007**, *4*, 164–167. [CrossRef]
69. Li, L.M.; Tang, H.N.; Lei, J.R.; Song, X.Q. Spatial autocorrelation in land use type and ecosystem service value in Hainan Tropical Rain Forest National Park. *Ecol. Indic.* **2022**, *137*, 108727. [CrossRef]
70. Zhou, S.C.; Wu, N.C.; Zhang, M.; Peng, W.Q.; He, F.Z.; Guo, K.; Yang, S.Y.; Zou, Y.; Qu, X.D. Local environmental, geo-climatic and spatial factors interact to drive community distributions and diversity patterns of stream benthic algae, macroinvertebrates and fishes in a large basin, Northeast China. *Ecol. Indic.* **2020**, *117*, 106673. [CrossRef]
71. Luo, Y.J.; Zhang, X.Q.; Wang, X.K.; Ren, Y. Dissecting Variation in Biomass Conversion Factors across China's Forests: Implications for Biomass and Carbon Accounting. *PLoS ONE* **2014**, *9*, e94777. [CrossRef]